Instabilities in a Stratified Fluid Having One Critical Level. Part I: Results

A. J. ROSENTHAL

Department of Mathematics, Massachusetts Institute of Technology, Cambridge, MA 02139

R. S. LINDZEN

Center for Earth and Planetary Physics, Harvard University, Cambridge, MA 02138

(Manuscript received 17 August 1981, in final form 21 October 1982)

ABSTRACT

We consider instabilities in a stratified Boussinesq fluid with basic velocity $U_0(z)$. We initiate this study by considering the detailed stability properties of a profile where $U_0(z)$ is constant in a top and bottom layer and varies linearly with z in an intermediate layer. For an infinite fluid, we find, in addition to Kelvin–Helmholtz instabilities similar to those found by Miles and Howard (1964), an unstable gravity wave mode propagating energy away from exactly one side of the shear zone if and only if the Richardson number in the shear zone is less than 0.1164 ± 0.0001. With a lower boundary present, we find gravity wave instabilities propagating above as well as below the shear zone can exist only when the Richardson number is less than 0.116. The ability of a shear zone to sustain instabilities propagating energy to infinity on one side is hence only present when the Richardson number is less than 0.116, whether or not the ground is present.

With a lower boundary present, we also find gravity wave instabilities evanescent above the shear zone for Richardson numbers up to 0.2499. After an exhaustive search involving varying the height of the shear zone above the ground and the wavenumber k, we conclude that, for any Richardson number less than ¼, the growth rates of gravity wave instabilities can be as much as, but not greater than, 26% of the maximal growth rates for Kelvin–Helmholtz instabilities having a critical level with the same Richardson number as the gravity wave instabilities have. Even though the relative importance of gravity wave instabilities can be significantly greater than found by other investigators (e.g., Davis and Peltier, 1976), the largest growth rates are still associated with Kelvin–Helmholtz instabilities.

In order to understand the basis for this behavior we will analyze, in subsequent parts, both types of instability in terms of wave overreflection. This will enable us to show that the relative importance of Kelvin–Helmholtz and gravity wave instabilities is by no means universal.

1. Introduction

The purpose of this paper is the development and presentation of the complete stability properties of the stratified shear flow shown in Fig. 1 with and without a lower boundary. In an earlier paper, Lindzen and Rosenthal (1976) find that the most unstable gravity waves associated with a Helmholtz velocity profile in a stably stratified fluid with a lower boundary present have several properties similar to those of disturbances observed in connection with clear air turbulence. However, they find that gravity waves have much smaller growth rates than Kelvin–Helmholtz instabilities and speculate that as the Richardson number (Ri) in the shear zone approaches ¼ from below, the most unstable gravity wave might have a growth rate larger than that of the Kelvin–Helmholtz instability for the same Ri.

In the present paper we find that the ratio of gravity wave to Kelvin–Helmholtz growth rates does increase as Ri varies from 0 to ¼, but only to a maximum ratio of 0.26. We also find the following:

1) Whereas the wavelength of the dominant Kelvin–Helmholtz instability increases as the thickness of the shear layer increases, the wavelength of the most unstable gravity wave remains relatively constant and close to wavelengths found in observations such as those of Ottersten *et al.* (1973) as Ri increases from 0 to ¼.

2) The wavelengths associated with the most unstable gravity wave and Kelvin–Helmholtz instabilities do approach each other as Ri increases to ¼.

3) The growth rates for gravity wave instabilities do have local maxima at preferred values of ground to shear layer distance when Ri is nonzero in the shear layer, as they do when Ri is 0 at the shear level.

4) As is the case for a Helmholtz velocity profile, gravity wave instabilities decay more slowly away from a shear layer with nonzero Ri than do Kelvin–Helmholtz instabilities and hence can be observable over a larger region.

Davis and Peltier (1976) consider a tanh-velocity profile for which the Richardson number at the in-

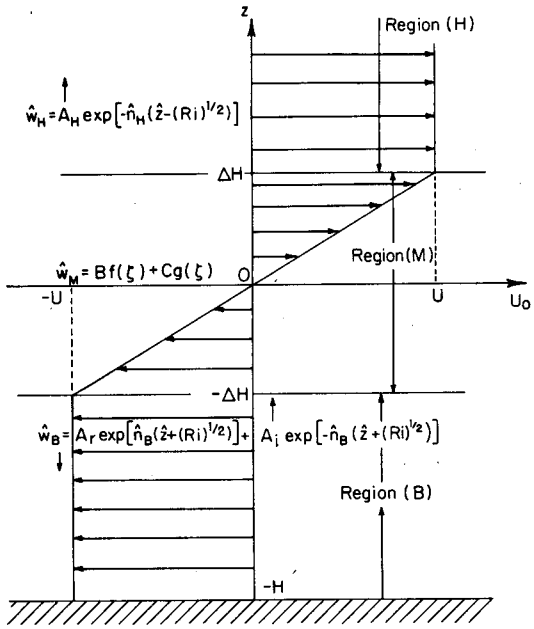

FIG. 1. Basic velocity profile having one critical layer. Also shown are the solutions for vertical velocity w in each layer.

flection point, a critical level for Kelvin–Helmholtz instabilities, is less than the Richardson number lower in the shear zone, where gravity wave instabilities have their critical level. With a region of large temperature gradient having the same depth as the region of large wind gradient around the inflection point [as in the case considered further by Davis and Peltier (1977, 1979)], they find that the maximal growth rate for gravity wave instabilities for a given Ri_{infl} at the inflection point is only 7% of the growth rate for Kelvin–Helmholtz instabilities at that Ri_{infl}. But, when considering the finite amplitude evolution of Kelvin–Helmholtz instabilities, Peltier *et al.* (1978) show that the velocity profile develops into one with a Richardson number greater at the original inflection point height than lower in the shear zone at the critical level for gravity wave instabilities. Now, we consider an intermediate broken-line profile with a constant Richardson number throughout the shear zone and find the growth rate for gravity wave instabilities can be over 25% of the growth rate for Kelvin–Helmholtz instabilities, a much larger value than the 7% ratio Davis and Peltier (1976) find. We raise the possibility that these results can be extrapolated to predict properties of the mean velocity profile Peltier *et al.* (1978) find to develop after smoothing by their finite amplitude Kelvin–Helmholtz waves. This extrapolation predicts that when Ri at the critical level is less for gravity wave instabilities than for Kelvin–Helmholtz instabilities, gravity wave instabilities could have comparable, or perhaps even larger, growth rates than Kelvin–Helmholtz instabilities associated with the same velocity profile. Whereas the intensified shears Peltier *et al.* (1978) find to develop in their mean velocity profile are not far enough from the shear zone to be consistent with multiple vertical layers observed in association with clear air turbulence (e.g., Atlas *et al.*, 1970), the gravity waves we find, which propagate in the region between the shear zone and the ground and have an integral number of half wavelengths there, could account for multiple layering in the vertical.

In Parts II and III we attempt to develop a deeper understanding of the numerical results of Part I. In Part II we explain the origin of our gravity wave instabilities in terms of overreflection, as was done by Lindzen and Rosenthal (1976) for the simpler Helmholtz profile. In Part III we show that the Kelvin–Helmholtz instability may also be thought of as resulting from multiple wave overreflection (of vorticity waves rather than gravity waves) within a region bounded between two turning point heights at which the character of the solution changes from propagating vertically to decaying vertically. As the horizontal wavenumber decreases to a small enough value that the lower turning point height for this Kelvin–Helmholtz mode goes down to the ground, this mode has properties indistinguishable from those of a gravity wave instability. This provides an explanation for the bifurcation of Kelvin–Helmholtz instabilities and gravity waves discussed by Lindzen and Rosenthal (1976). An alternative to thinking of these gravity waves as analytic continuations of the Kelvin–Helmholtz mode is to think of the Kelvin–Helmholtz instability as generated, as is the gravity wave instability, by overreflection between a critical level and a lower level: the ground for gravity wave instabilities and the internal lower turning point height for Kelvin–Helmholtz instabilities. Because gravity waves must propagate a greater distance vertically between overreflections than vorticity waves, gravity waves generally have smaller growth rates than Kelvin–Helmholtz instabilities (when both are generated at critical layers having the same Richardson number).

However, the insights gained in Parts II and III allow us in a subsequent article (Rosenthal and Lindzen, 1983) to show that reasonable profiles can exist which display only gravity wave instabilities and no Kelvin–Helmholtz instabilities.

2. Model and equations

We consider the behavior of small two-dimensional perturbations of the form $f' = f(z)\exp[ik(x - ct)]$ on a basic state consisting of a Boussinesq fluid with a constant Brunt–Väisälä frequency N, given by

$$N^2 = \frac{g}{\rho_0(z)}\frac{d\rho_0}{dz}, \tag{1}$$

where $\rho_0(z)$ is the basic density distribution, g gravi-

tational acceleration, x horizontal distance, z height and t time. The linearized equations for such perturbations are

$$\frac{\partial u'}{\partial t} + U_0(z)\frac{\partial u'}{\partial x} + w'\frac{\partial U_0(z)}{\partial z} = -\frac{1}{\rho_0}\frac{\partial p'}{\partial x}, \quad (2)$$

$$\frac{\partial w'}{\partial t} + U_0(z)\frac{\partial w'}{\partial x} = -\frac{1}{\rho_0}\frac{\partial p'}{\partial z} - \frac{g\rho'}{\rho_0}, \quad (3)$$

$$\frac{\partial \rho'}{\partial t} + U_0(z)\frac{\partial \rho'}{\partial x} + w'\frac{d\rho_0}{dz} = 0, \quad (4)$$

$$\frac{\partial u'}{\partial x} + \frac{\partial w'}{\partial z} = 0, \quad (5)$$

where u' and w' are the horizontal and vertical velocity perturbations, respectively; p' is the pressure perturbation; ρ' the density perturbation; and $U_0(z)$ is the basic velocity profile shown in Fig. 1. $U_0(z) = -U$ if $z < -\Delta H$, $U_0(z) = zU/\Delta H$ if $-\Delta H < z < \Delta H$, and $U_0(z) = U$ if $z > \Delta H$. Except for the additional term $w'\partial U_0(z)/\partial z$ in (2), the above equations are the same as used by Lindzen (1974). We now obtain

$$\Phi \equiv \frac{p}{\rho_0} = \frac{[U_0(z) - c]}{ik}\frac{dw}{dz} - \frac{w}{ik}\frac{dU_0(z)}{dz}, \quad (6)$$

$$\frac{d^2w}{dz^2} - n^2(z)w = 0, \quad (7)$$

where

$$n^2(z) = k^2 - \left[\frac{N}{U_0(z) - c}\right]^2 + \frac{d^2U_0(z)/dz^2}{U_0(z) - c}. \quad (8)$$

The solution in region H is

$$w_H = A_H \exp[-n_H(z - \Delta H)], \quad (9)$$

where n_H is the square root of $k^2 - [N/(U - c)]^2$ having $\mathrm{Re}(n_H) \geq 0$ if $c_i \geq 0$ and $(\mathrm{Im}n_H)(c_r - U) \geq 0$, where $c = c_r + ic_i$ (by the radiation condition). In region B, the solution is

$$w_B = A_r \exp[n_B(z + \Delta H)] + A_i \exp[-n_B(z + \Delta H)], \quad (10)$$

where n_B is the square root of $k^2 - [N/(U + c)]^2$ having $\mathrm{Re}(n_B) \geq 0$ if $c_i \geq 0$ and $(\mathrm{Im}n_B)(c_r + U) \geq 0$. Then, if $\mathrm{Re}(n_B) = 0$, $A_r \exp[n_B(z + \Delta H)]$ represents a reflected wave having energy flux propagating away from the shear layer and $A_i \exp[-n_B(z + \Delta H)]$ represents an incident wave carrying energy toward the shear layer. This incident wave would not be present without the lower boundary.

As done by Lindzen and Rosenthal (1976), we define the following nondimensional variables:

$$\left.\begin{aligned} \hat{n} &= nU/N, \quad \hat{k} = kU/N, \quad \hat{c} = c/U, \quad \hat{w} = w/U \\ \hat{H} &= HN/U, \quad \hat{z} = zN/U, \quad \hat{\omega} = \omega/N = kc/N \end{aligned}\right\}.$$

Also, the Richardson number is defined for region M as

$$\mathrm{Ri} = \frac{N^2}{\left(\frac{dU_0}{dz}\right)^2} = \frac{(\Delta H)^2N^2}{U^2}. \quad (11)$$

In region M, where $U_0(z)/U = z/\Delta H = \hat{z}/(\mathrm{Ri})^{1/2}$, Eq. (7) becomes

$$\frac{d^2\hat{w}}{d\zeta^2} + \left(\frac{\mathrm{Ri}}{\zeta^2} - 1\right)\hat{w} = 0, \quad (12)$$

where

$$\zeta = \hat{k}(\mathrm{Ri})^{1/2}[U_0(z)/U - \hat{c}]. \quad (13)$$

When $0 < \mathrm{Ri} < \frac{1}{4}$, the solution to (12) may be written

$$\hat{w} = Bf(\zeta) + Cg(\zeta), \quad (14)$$

where

$$f(\zeta) = \zeta^{m+1/2}\sum_{j=0}^{\infty}\left(\frac{\zeta}{2}\right)^{2j}[j!\prod_{k=1}^{j}(k+m)]^{-1} = 2^m\zeta^{1/2}\Gamma(1+m)I_m(\zeta), \quad (15a)$$

$$g(\zeta) = \zeta^{1/2-m}\sum_{j=0}^{\infty}\left(\frac{\zeta}{2}\right)^{2j}[j!\prod_{k=1}^{j}(k-m)]^{-1} = 2^{-m}\zeta^{1/2}\Gamma(1-m)I_{-m}(\zeta), \quad (15b)$$

where $m = (\frac{1}{4} - \mathrm{Ri})^{1/2}$,

$$\prod_{k=1}^{j} a_k = a_1a_2a_3\cdots a_j \quad \text{if} \quad j \geq 1, \quad \prod_{k=1}^{0} a_k = 1,$$

and I is the "Bessel function of imaginary argument" (Goldstein, 1931). Note that $|U_0(z)/U - \hat{c}| < 1$ for unstable waves by the semicircle theorem (Howard, 1961). For $0 < \mathrm{Ri} < \frac{1}{4}$ and $\hat{k} < 2$ for cases of interest, we have $|\zeta| < 2$. Then, 14 terms are sufficient to evaluate the power series in (15) for $f(\zeta)$, $g(\zeta)$, $f'(\zeta)$, and $g'(\zeta)$ (obtained by differentiating term by term) to better than 12 decimal places. As explained by Booker and Bretherton (1967), the branch needed to evaluate the fractional powers of ζ in (15) is the one on which $-\pi \leq \theta \leq 0$ for $c_i \geq 0$, where $\theta = \arg\zeta$. Then, $\zeta^P = |\zeta|^P e^{iP\theta}$.

At the interfaces between the different regions in Fig. 1, we require continuity of pressure and vertical displacement. These matching conditions imply continuity of Φ [given by (6)], and of w, since $U_0(z)$ is continuous for the velocity profiles considered now. Using our matching conditions and the condition that $\hat{w}(-\hat{H}) = 0$ at the fixed lower boundary, we find that

$$A_H - f(\zeta_1)B - g(\zeta_1)C = 0, \quad (16a)$$

$$t_1A_H + [f(\zeta_1) - \zeta_1f'(\zeta_1)]B + [g(\zeta_1) - \zeta_1g'(\zeta_1)]C = 0, \quad (16b)$$

$$f(\zeta_2)B + g(\zeta_2)C - A_r - A_i = 0, \quad (17a)$$

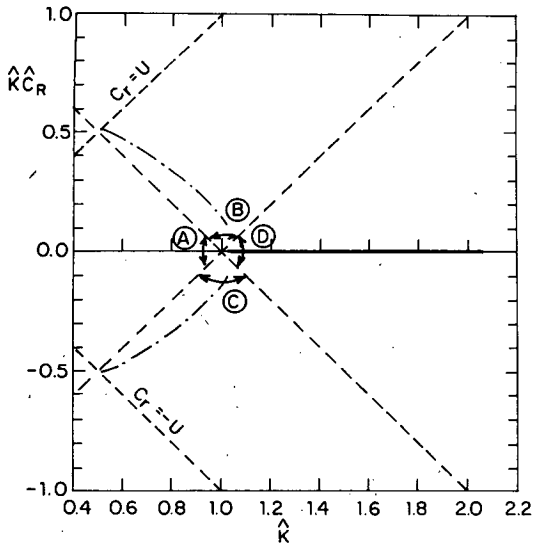

FIG. 2. Nondimensional frequency $\hat{k}\hat{c}_r$ versus $\hat{k}$ for instabilities when Ri = 0.10 in an unbounded fluid. The dashed curve represents a gravity wave instability just propagating either above $z = \Delta H$ (in region B) or below $z = -\Delta H$ (in region C). The solid curve is a Kelvin–Helmholtz instability decaying both above and below the shear zone. (Such waves are in region D.)

$$[f(\zeta_2) - \zeta_2 f'(\zeta_2)]B + [g(\zeta_2) - \zeta_2 g'(\zeta_2)]C - t_2 A_r + t_2 A_i = 0, \quad (17b)$$

$$\exp[2\hat{n}_B(\mathrm{Ri}^{1/2} - \hat{H})]A_r + A_i = 0, \quad (18)$$

where, at $z = \Delta H$,

$$\zeta_1 = \hat{k}(\mathrm{Ri})^{1/2}(1 - \hat{c}), \quad t_1 = \hat{n}_H(\mathrm{Ri})^{1/2}(\hat{c} - 1), \quad (19)$$

and, at $z = -\Delta H$,

$$\zeta_2 = -\hat{k}(\mathrm{Ri})^{1/2}(1 + \hat{c}), \quad t_2 = \hat{n}_B(\mathrm{Ri})^{1/2}(\hat{c} + 1). \quad (20)$$

3. Solutions for an unbounded fluid with one critical level

For an unbounded fluid, $A_i = 0$ and (16) and (17) give the dispersion relation

$$h_1 = 0, \quad (21)$$

where

$$h_1 = a_2 a_3 - a_1 a_4, \quad (22)$$

$$a_1 = \zeta_1 f'(\zeta_1) - (1 + t_1) f(\zeta_1), \quad (23)$$

$$a_2 = \zeta_1 g'(\zeta_1) - (1 + t_1) g(\zeta_1), \quad (24)$$

$$a_3 = -\zeta_2 f'(\zeta_2) + (1 - t_2) f(\zeta_2), \quad (25)$$

$$a_4 = -\zeta_2 g'(\zeta_2) + (1 - t_2) g(\zeta_2). \quad (26)$$

The same two-dimensional secant method as used by Lindzen and Rosenthal (1976) can be used to solve (21). The disturbances having the largest growth rates now are Kelvin–Helmholtz instabilities with properties closely resembling those found for the Kelvin–Helmholtz mode when a lower boundary is present at a distance greater than $\hat{H} = 2$ below the shear layer, as will be described next.

Whereas neutral gravity waves propagating energy away from the shear zone both upwards and downwards are found by Lindzen (1974) for an infinite fluid with Ri = 0 at the critical level, no such propagating gravity waves are found now. However, we do find an unstable gravity wave mode propagating energy away from one side of the shear zone if and only if the Richardson number in the shear zone is less than 0.1164 ± 0.0001. On the other side of the shear zone (i.e., above the shear zone for $c_r < 0$ and below the shear zone for $c_r > 0$), this gravity wave instability decays exponentially with vertical distance from the shear zone. In Figs. 2 and 3, we show the frequency $\hat{k}\hat{c}_r$ and growth rate $\hat{k}\hat{c}_i$ for both the Kelvin–Helmholtz and this gravity wave mode when Ri = 0.10. We note that the gravity wave's maximal growth rate is only 7.4% of the Kelvin–Helmholtz mode's maximal growth rate. As the Richardson number in the shear zone approaches 0.1164 from below, the gravity wave mode is most unstable for a horizontal wavenumber of $\hat{k} = 0.933$; then the vertical wavenumber is $\mathrm{Im}(\hat{n}) = \mathrm{Im}(nU/N) = 0.931$ on the side of the shear zone in which there is vertical propagation. These wavenumbers are similar to the wavenumber of $\hat{k} = 2^{-1/2} = 0.707\ldots$ found by Lindzen (1974) to be most efficient at carrying energy away from a shear level at which Ri = 0. When Ri > 0, this apparent infinite overreflection (with a wave propagating vertically away from the shear zone even though there is no incident wave) may be explained

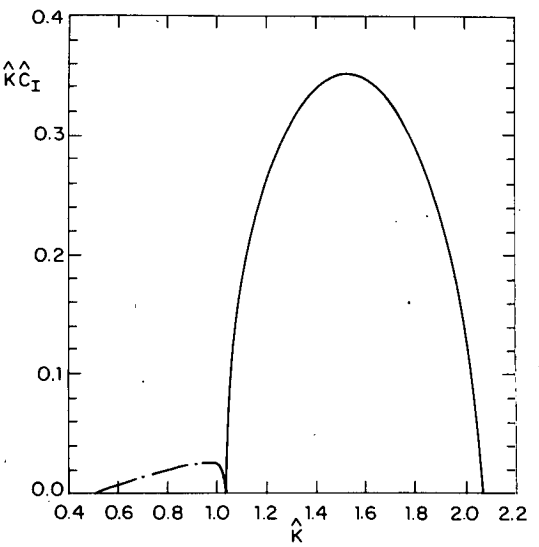

FIG. 3. Nondimensional growth rate $\hat{k}\hat{c}_i$ versus $\hat{k}$ when Ri = 0.10 in an unbounded fluid. The dashed curve represents a gravity wave instability and the solid curve is a Kelvin–Helmholtz instability.

in terms of wave overreflection by considering a subduct in the shear layer between the critical level at which $c_r = U$ and the turning point at which $[N/(U_0(z) - c_r)]^2 - k^2 = 0$. Multiple overreflection occurs between these two levels and, as long as Ri < 0.1164, the waves can extract energy from the mean flow (due to overreflection at the critical level) at a rate sufficiently larger than the rate of leakage of energy away from the shear zone by the propagating gravity waves that an instability can be sustained. The disappearance of this gravity wave instability when Ri > 0.1164 is related to the nonexistence of gravity wave instabilities propagating above as well as below the shear zone in a semi-infinite fluid when Ri > 0.116, as will be noted in the next section.

These results are comparable to those of Jones (1968), who finds two instability surfaces for a similar model, but without the Boussinesq approximation. Jones (1968) finds one instability has a singular neutral mode at large wavenumbers which is evanescent in both bounding half-spaces. The singular neutral modes he finds at small wavenumbers bounding the other instability surface are decaying in one half-space. Thus, Jones' first solution can correspond to our Kelvin–Helmholtz instability and his second solution corresponds to our gravity wave instability.

4. Solutions for a semi-infinite fluid with one critical level

With the ground present at a distance $\hat{H} = HN/U$ below the center of the shear layer, Eqs. (16), (17) and (18) give the dispersion relation

$$h_1 + h_2 \exp[2\hat{n}_B(\mathrm{Ri}^{1/2} - \hat{H})] = 0, \qquad (27)$$

where

$$h_2 = a_1 a_8 - a_2 a_7, \qquad (28)$$

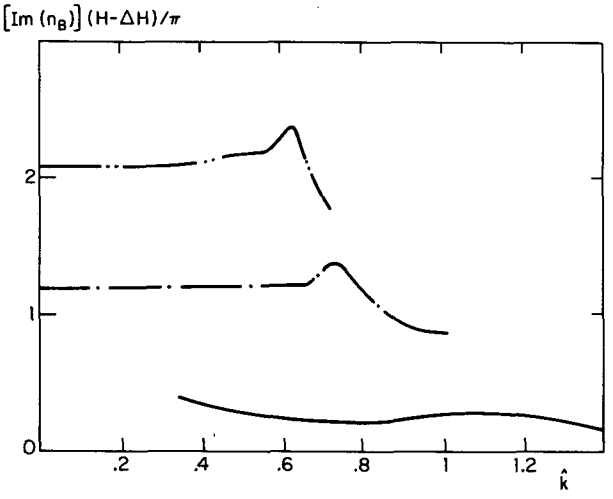

FIG. 4. Mode number versus $\hat{k}$ when $\hat{H} = 3.24$ and Ri = 0.05 in the shear layer. Modes $M = 1$ and $M = 2$ and the Kelvin–Helmholtz instability (solid line) are shown.

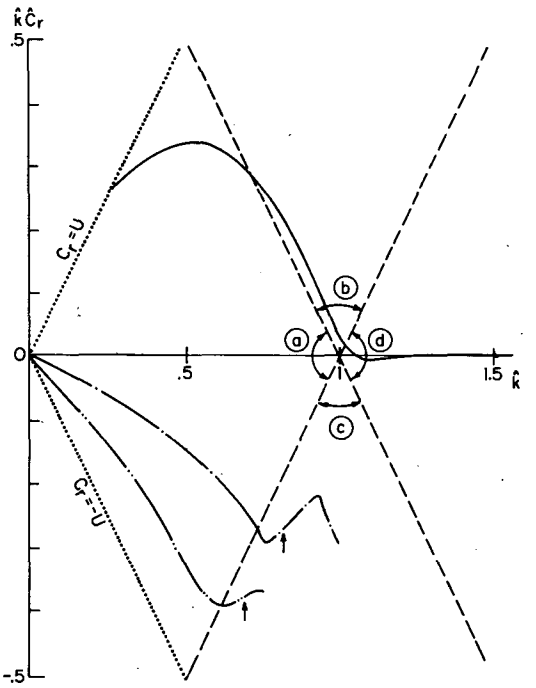

FIG. 5. Nondimensional frequency $\hat{k}\hat{c}_r = kc_r/N$ versus $\hat{k}$ when $\hat{H} = 3.24$ and Ri = 0.05. The solid line represents the Kelvin–Helmholtz instability. Curves with a dash followed by M dots represent gravity wave instabilities of mode number M. Vertical arrows indicate the wavenumbers of maximal growth rate.

$$a_7 = -\zeta_2 f'(\zeta_2) + (t_2 + 1) f(\zeta_2), \qquad (29)$$

$$a_8 = -\zeta_2 g'(\zeta_2) + (t_2 + 1) g(\zeta_2), \qquad (30)$$

and other quantities have the same definition as in Sections 2 and 3.

As is the case when Ri = 0 (Lindzen and Rosenthal, 1976), Eq. (27) has one Kelvin–Helmholtz mode plus an infinite sequence of unstable gravity wave modes as solutions. For the gravity wave instabilities, the number of vertical wavelengths between the bottom of the shear layer at $\hat{z} = -(\mathrm{Ri})^{1/2}$ and the lower boundary at $\hat{z} = -\hat{H}$ is quantized to have discrete values close to $M/2$, where $M = 1, 2, 3, \ldots$. Henceforth, this quantity M, which is approximately $\mathrm{Im}(\hat{n}_B)[\hat{H} - (\mathrm{Ri})^{1/2}]\pi^{-1} = \mathrm{Im}(n_B)[H - \Delta H]\pi^{-1}$ (see Fig. 4) is called the mode number of the instability.

As shown by Figs. 5 and 6 for a typical case with $\hat{H} = 3.24$, when Ri = 0.05, gravity wave instabilities exist both in region A of $(\hat{k}, \hat{k}\hat{c}_r)$ space (where they propagate vertically both above and below the shear layer) and in region C of $(\hat{k}, \hat{k}\hat{c}_r)$ space (where they are trapped above the shear layer). Whereas when $0 \leqslant \mathrm{Ri} \leqslant 0.02$, the most unstable gravity wave is found in region A, we find that when $0.03 \leqslant \mathrm{Ri} < 0.25$, the most unstable gravity wave is found in region C. Although the maximal gravity wave growth rate is only 18% of that for the Kelvin–Helmholtz

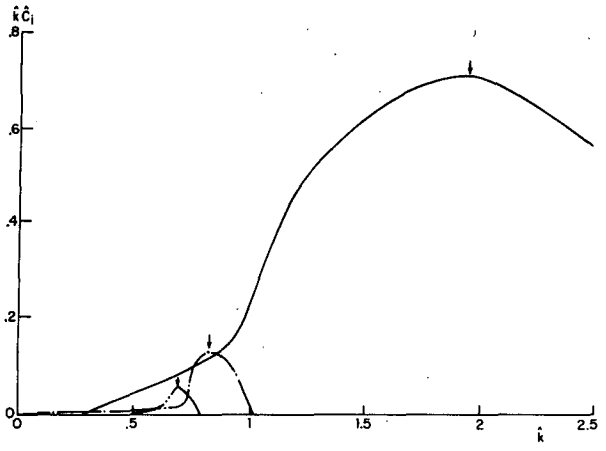

FIG. 6. Growth rate $\hat{k}\hat{c}_i$ versus horizontal wavenumber $\hat{k}$ when $\hat{H} = 3.24$ and Ri = 0.05 in the shear layer. See Fig. 5 for the curve-labeling convention used.

instability when Ri = 0.05, gravity waves are consistent with observations of layered structures extending far from the shear zones. Such modes may be observable because their exponential decay rate in z is much smaller than that of Kelvin–Helmholtz waves.

When Ri $\gtrsim$ 0.116 in the shear zone (as is illustrated by Figs. 7 and 8 for Ri = 0.15 and $\hat{H} = 3.24$), there no longer are any instabilities in region A of ($\hat{k}$, $\hat{k}\hat{c}_r$) space that propagate above as well as below the shear zone. Then, the amplification of gravity waves due to a sequence of reflections at the ground is not capable of compensating for the leakage of energy that would occur above the shear zone by an upward propagating gravity wave there. Since there is only partial reflection at the critical level of gravity waves that would propagate above $z = \Delta H$ when Ri $\gtrsim$ 0.116 (as will be discussed in more detail in Part II), instabilities propagate at most in the layer between the shear zone and the ground when Ri $\gtrsim$ 0.116. As Figs. 9a and 9b show, gravity wave instabilities have much slower exponential decay in z below the shear zone but only slightly slower exponential decay in z above the shear zone than the Kelvin–Helmholtz instability. These gravity wave instabilities propagating vertically just in the duct between the ground and the shear layer with Ri $\gtrsim$ 0.116 are important because their momentum flux comes from the shear but cannot leave; hence, their wave flux is available to maintain the shear, as explained by Lindzen and Rosenthal (1976).

Figs. 10 and 11 show, for the sample case $\hat{H} = 3.24$, that gravity waves and Kelvin–Helmholtz instabilities coexist for Richardson numbers ranging from 0 to 0.2499, with gravity waves at any given Ri having growth rates several times less than the most unstable Kelvin–Helmholtz instability at that Ri. At Ri = 0.2499 and $\hat{H} = 3.24$, the fastest growing gravity wave instability (now the $M = 1$ mode) has a growth rate that is 24% that of the fastest growing Kelvin–Helmholtz instability for these parameters.

The Kelvin–Helmholtz mode shown in Figs. 10 and 11 has properties differing by less than 2% from those of the Kelvin–Helmholtz mode in an unbounded fluid discussed in Section 3. Its exponential decay over a height of $\hat{H} = 3.24$ is sufficiently great that the presence of a lower boundary does not modify it significantly. However, these Kelvin–Helmholtz

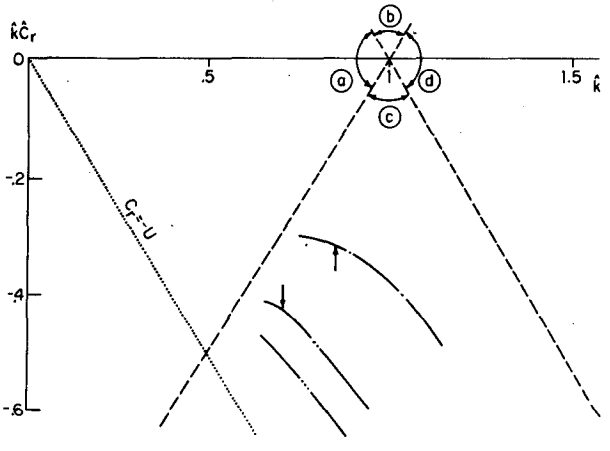

FIG. 7. Nondimensional frequency $\hat{k}\hat{c}_r = kc_r/N$ versus $\hat{k}$ when $\hat{H} = 3.24$ and Ri = 0.15 in the shear layer. See Fig. 5 for the curve-labeling convention.

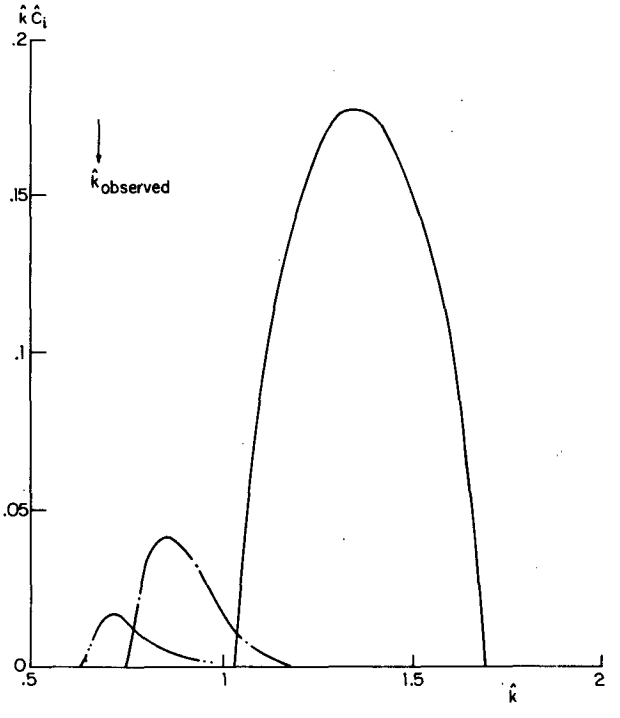

FIG. 8. Growth rate $\hat{k}\hat{c}_i = kc_i/N$ versus $\hat{k}$ when $\hat{H} = 3.24$ and Ri = 0.15 in the shear layer. See Fig. 5 for the curve-labeling convention.

modes differ more and more from those described by Miles and Howard (1964) as the Richardson number increases. At larger Ri = $N^2/(dU_0/dz)^2$, the lack of stratification outside the shear zone in Miles and Howard's (1964) work makes their model differ more significantly from ours, in which stratification extends beyond the shear zone. (Of course, the main modification to earlier results introduced by the presence of stratification outside the shear zone is that vertically propagating gravity waves can now be present).

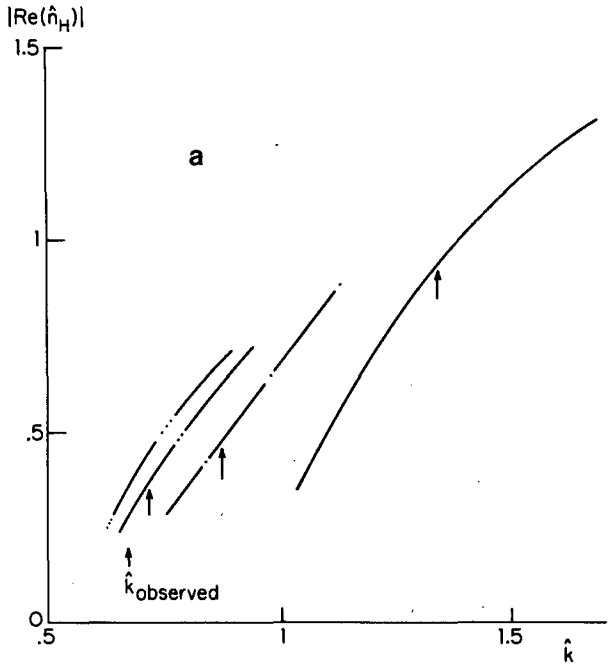

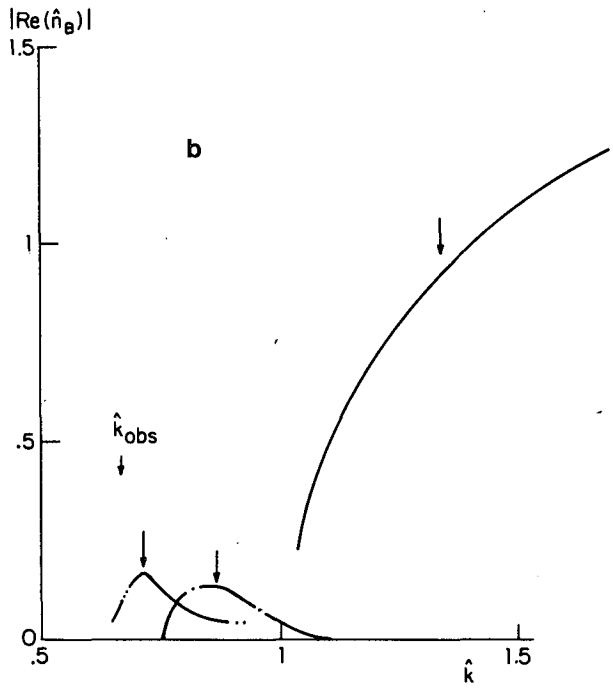

FIG. 9. Exponential decay rate in $\hat{z}$ versus $\hat{k}$ when $\hat{H}$ = 3.24 and Ri = 0.15 for (a) the upper region above the shear layer and (b) the bottom region between the shear layer and the ground. See Fig. 5 for the curve-labeling convention.

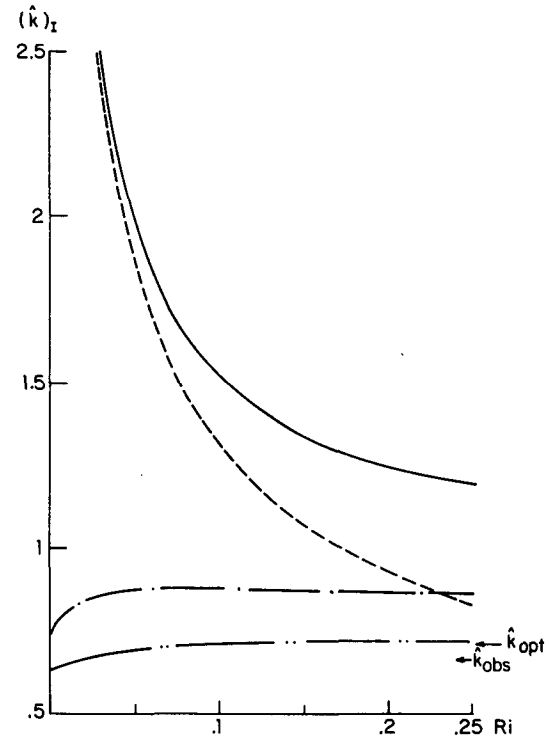

FIG. 10. Most unstable wavenumbers versus Ri when $\hat{H}$ = 3.24 (as in Case 2 of Lindzen, 1974). The dashed curve shows the wavenumber of the most unstable Kelvin–Helmholtz instability found by Miles and Howard (1964) for an infinite fluid stratified only in the shear layer. See Fig. 5 for the curve-labeling convention for the gravity wave instabilities.

We find that gravity wave instabilities exist at all Richardson numbers up to 0.2499, which is very close to the theoretical upper bound of ¼ established by Miles (1961). Comparing this result with Davis and Peltier's (1976) conclusion that the Richardson number at the height of the inflection point in the wind profile must be significantly less than ¼ (apparently less than 0.22 from their Figs. 13 and 14) before gravity wave instabilities appear is worthwhile. This comparison shows that the Richardson number at the critical level where $U_0(z_c) = c_r$, instead of the minimum Richardson number in the flow, is the more important parameter. Since gravity waves must have $c_r < 0$ to be overreflected when Ri > 0.116 (see Part II) and Ri (z = 0) < Ri(z_c) for waves with $c_r < 0$ in a hyperbolic tangent velocity profile, unstable gravity wave modes can disappear even though Ri (z = 0) is still significantly less than ¼ but Ri(z_c) has reached ¼. With our broken line profile, Ri is constant throughout the shear zone, and even when $c_r \neq 0$, as

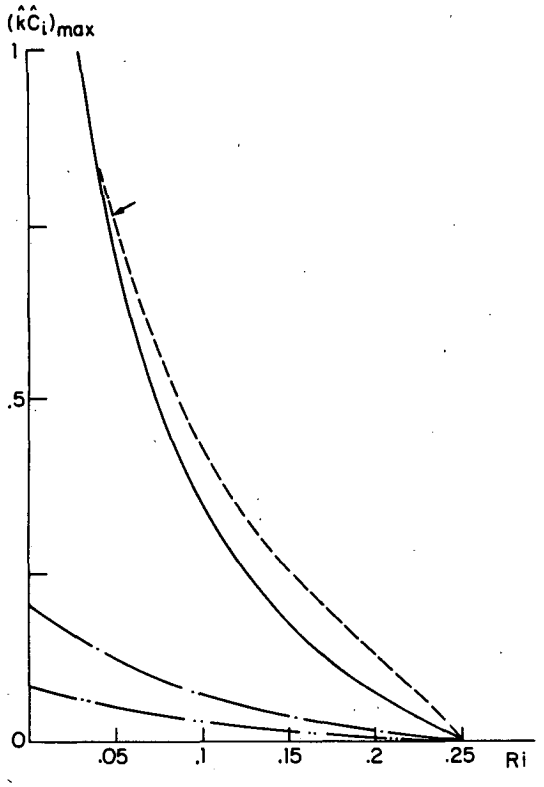

FIG. 11. Maximum growth rate versus Ri when $\hat{H} = 3.24$ (as in Case 2 of Lindzen, 1974). The dashed curve represents the most unstable instability according to Miles and Howard (1964) for an infinite fluid stratified only in the shear layer. See Fig. 5 for the curve-labeling convention for the gravity wave instabilities.

is typically the case for gravity wave instabilities, we have Ri ($z = 0$) = Ri ($z = z_c$). Hence, Ri ($z = 0$) and Ri ($z = z_c$) reach the upper bound at which instabilities can be present, i.e., ¼, simultaneously.

Although Fig. 11 does show that, when $\hat{H} = 3.24$, the most unstable Kelvin–Helmholtz mode at any given Ri ≤ 0.2499 has a growth rate $\max_{\hat{k}}(\hat{k}\hat{c}_i)_{KH}$ over four times larger than the largest growth rate $\max_{\hat{k}}(\hat{k}\hat{c}_i)_g$ of any gravity wave instability at that Ri, a more exhaustive search over both the parameters Ri and $\hat{H}$ is admittedly necessary to establish that, for any given Ri and $\hat{H}$, gravity wave instabilities are always less unstable than the most unstable Kelvin–Helmholtz instabilities. As Fig. 12 shows for the sample case Ri = 0.24, $\max_{\hat{k}}(\hat{k}\hat{c}_i)_g$ depends on $\hat{H}$ and has a maximum at $\hat{H} = 3.79$. The wavenumber of maximal instability of gravity wave modes, shown in Fig. 13, remains for all $\hat{H} > 5$ within 10% of the most unstable wavenumber for the gravity wave instability in an unbounded fluid with Ri = 0.24 in the shear layer. The associated vertical wavenumber between the shear zone and the ground for this gravity wave instability comes closest to satisfying the quantization condition discussed earlier only at a certain value of $\hat{H}$. At that $\hat{H}$, we find $\max_{\hat{k},\hat{H}}(\hat{k}\hat{c}_i)_g$ for gravity wave instabilities for the value of Ri being considered. On the other hand, $\max_{\hat{k}}(\hat{k}\hat{c}_i)_{KH}$ (the maximum growth rate of the Kelvin–Helmholtz mode at a given $\hat{H}$) is relatively insensitive to variations of $\hat{H}$, except for values of $\hat{H}$ less than 2, which are smaller than those values of $\hat{H}$ typically observed in the atmosphere. (With a lower Brunt–Väisälä frequency in the layer below the shear zone than in the shear zone, these smaller values of $\hat{H}$ might perhaps be realizable).

As shown by Fig. 12, the maximal growth rate of gravity wave instabilities, $\max_{\hat{k},\hat{H}}(\hat{k}\hat{c}_i)_g$ (Ri = 0.24), is several times smaller than the maximal growth rate of the Kelvin–Helmholtz instability, $\max_{\hat{k}}(\hat{k}\hat{c}_i)_{KH}$ at that height $\hat{H} = 3.79$ for which $\max_{\hat{k},\hat{H}}(\hat{k}\hat{c}_i)_g$ is attained. The growth rates of gravity wave instabilities decrease to 0 as $\hat{H}$ decreases to $(\text{Ri})^{1/2}$. As noted by Lindzen and Rosenthal (1976), the vertical wavelength of a gravity wave instability having $M/2$ vertical wavelengths between the ground and the shear zone (where M is quantized to be close to an integer $+¼$) must decrease as $\hat{H}$ decreases to $(\text{Ri})^{1/2}$ until the vertical wavelength is much less than that for the gravity wave most efficient at extracting energy from the shear zone. Then, $c_r \rightarrow -U$ and the reflection coef-

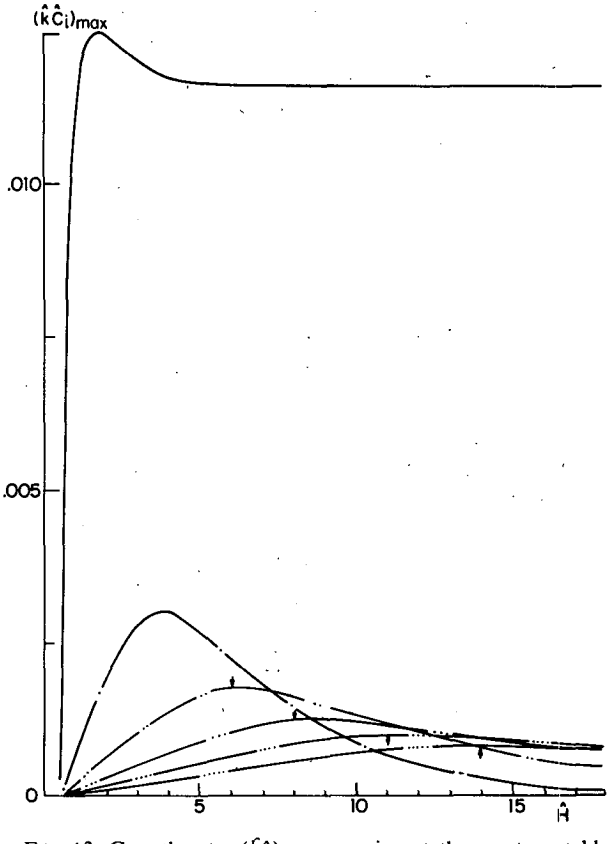

FIG. 12. Growth rates $(\hat{k}\hat{c}_i)_{max}$ occurring at the most unstable wavenumbers $\hat{k}_l$ for a given mode versus $\hat{H}$ when Ri = 0.24 in the shear layer. See Fig. 5 for the curve-labeling convention for the gravity wave instabilities.

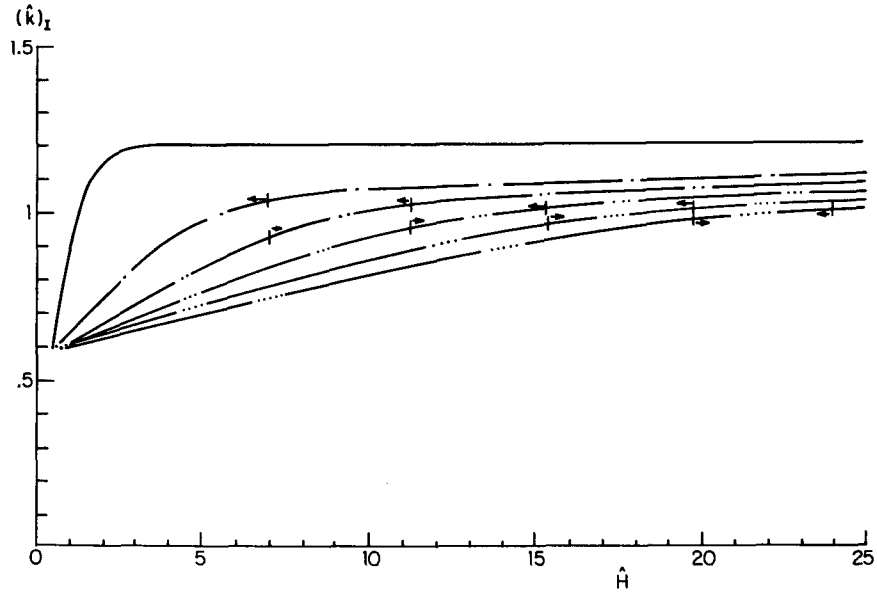

FIG. 13. Wavenumber $\hat{k}_I$ having maximal growth rate versus $\hat{H}$ when Ri = 0.24 in the shear layer. See Fig. 5 for the curve-labeling convention. The horizontal arrows denote the range of wavenumbers for which the indicated gravity wave mode is the most unstable mode.

ficient R_w (as defined by Lindzen and Rosenthal, 1976) decreases to 1. This will be shown in Part II.

Besides explaining why the gravity wave modes have smaller growth rates as $\hat{H}$ becomes very small, the previous argument can explain the reduced growth rate for the Kelvin–Helmholtz mode as $\hat{H}$ decreases to $(\mathrm{Ri})^{1/2}$. [Similar stabilization of the Kelvin–Helmholtz mode when boundaries are close to the shear zone has also been described by Hazel (1972).] We first note that for small $\hat{H}$, the wavenumber of maximal instability for the Kelvin–Helmholtz mode decreases to a wavenumber more typical of a gravity wave instability (see Fig. 13). It turns out that this instability now occurs in region C of $(\hat{k}, \hat{k}\hat{c}_r)$ space (as in Fig. 5) and is vertically propagating between the bottom of the shear zone and the ground. It does not decay appreciably in traveling from the shear zone down to the ground, and has properties similar to those of a gravity wave instability. Hence, the growth rate of this mode also decreases to 0 as $\hat{H}$ decreases to $(\mathrm{Ri})^{1/2}$ and c_r decreases to $-U$.

The Kelvin–Helmholtz mode also has a growth rate which has a maximum at a particular value of $\hat{H}$. This previously unremarked property of the Kelvin–Helmholtz mode, which is barely noticeable for Ri = 0.116 or smaller, is clearly noticeable in Fig. 12, for Ri = 0.24. At $\hat{H} = 1.7$ and $\hat{k} = 1.11$, the maximal growth rate of the Kelvin–Helmholtz mode for Ri = 0.24 is $\max_{\hat{k},\hat{H}}(\hat{k}\hat{c}_i)_{\mathrm{KH}} = 0.0125$, a value which is 7.8% larger than the maximal growth rate of $\max_{\hat{k}}(\hat{k}\hat{c}_i)_{\mathrm{KH}} = 0.0116$ that the Kelvin–Helmholtz mode has at $\hat{k} = 1.21$, as $\hat{H} \to \infty$. Perhaps the enhanced growth rate of the Kelvin–Helmholtz instability at $\hat{H} = 1.7$ may be explained by the mechanism of multiple overreflection occurring between its critical level and its lower turning point below which it is evanescent rather than propagating vertically. The subduct resulting from this mechanism will be described quantitatively in Part III.

To explore the possibility that, for some Richardson numbers (Ri) in the shear layer, the maximal growth rate for gravity wave instabilities, $\max_{\hat{k},\hat{H}}(\hat{k}\hat{c}_i)_g$, could be larger than $\max_{\hat{k},\hat{H}}(\hat{k}\hat{c}_i)_{\mathrm{KH}}$ for Kelvin–Helmholtz instabilities at that Ri, we could search for that $\hat{H}$ that maximizes $\max_{\hat{k}}(\hat{k}\hat{c}_i)_g$ (as tabulated in graphs such as Fig. 12, where values of $\max_{\hat{k}}(\hat{k}\hat{c}_i)_g$ may each be determined from graphs such as Fig. 8), with Ri a parameter varying between 0.05 and 0.2499. We find that results from such a search agree with those found by simultaneously maximizing $\hat{k}\hat{c}_i$ with respect to $\hat{k}$ and $\hat{H}$ using a version of Powell's method (Walsh, 1975). The mode 1 gravity-wave instability has a maximal growth rate, $\max_{\hat{k},\hat{H}}(\hat{k}\hat{c}_i)_g$, occurring when the ground to center of shear layer distance, $\hat{H}_g$, has the values shown in Fig. 14.

As Fig. 15 indicates, the wavenumber $\hat{k}_g$ for which gravity wave instabilities have the largest growth rate at $\hat{H}_g$ remains relatively constant as the Richardson number varies from 0.05 to 0.25. This behavior contrasts with that of the Kelvin–Helmholtz instability, whose most unstable wavenumber is inversely proportional to the thickness ΔH of the shear layer (Miles and Howard, 1964), which in turn is proportional to $(\mathrm{Ri})^{1/2}UN^{-1}$. This confirms the conjecture by Lindzen and Rosenthal (1976) that the wavelength of the dom-

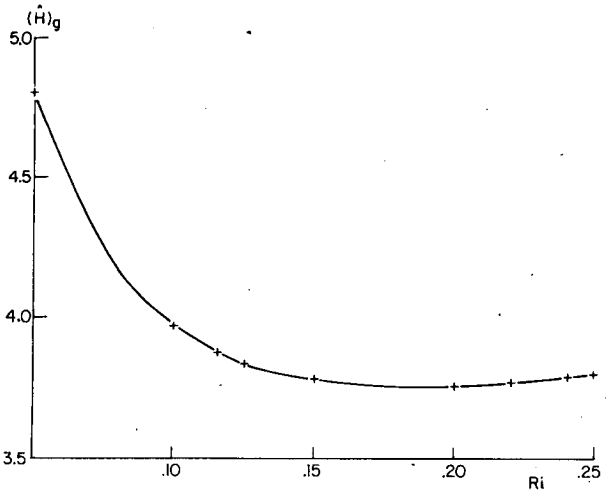

FIG. 14. Values of $\hat{H}_g$ for which gravity wave instabilities have their largest growth rates $(\hat{k}\hat{c}_i)_g$ (for all $\hat{H}$ and $\hat{k}$) as a function of the Richardson number (Ri) in the shear zone.

inant gravity-wave instability, which was calculated at Ri = 0 to be close to the observed wavelength, would remain close to the observed wavelength independent of the thickness of the shear layer, $2\Delta H$. In this respect, gravity wave instabilities are more consistent with constant wavelengths observed over intervals greater than 10 minutes as a shear layer is smoothed (Hooke *et al.*, 1973) than are Kelvin-Helmholtz instabilities, whose wavelength would increase proportionally to $2\Delta H$. Still, even at the ground to shear layer distance $\hat{H}_g$ for which the fastest growing gravity wave instability is found, its growth rate is less than that of a Kelvin-Helmholtz instability at the same Ri, as is shown by Fig. 16. It is possible to show that the excitation of about the same gravity wave wavelength throughout the smoothing of the shear zone causes a relative enhancement of gravity waves compared to Kelvin-Helmholtz instabilities (whose fastest growing wavelength changes during the smoothing of the shear zone) from what would be expected due to comparing growth rates only; i.e., the most unstable gravity wave remains such through the entire smoothing cycle in contrast to the behavior of Kelvin-Helmholtz instabilities. Although the growth rate for Kelvin-Helmholtz instabilities remains greater than that for the most unstable gravity wave (even at its preferred value of $\hat{H}_g$) as the Richardson number approaches ¼ from below, we see from Fig. 17 that the ratio of maximal growth rates for gravity waves to maximal growth rates for Kelvin-Helmholtz instabilities increases from 0 at Ri = 0 (Lindzen and Rosenthal, 1976) to 0.26 at Ri = ¼. These points are moot for profiles which have *only* gravity wave in-

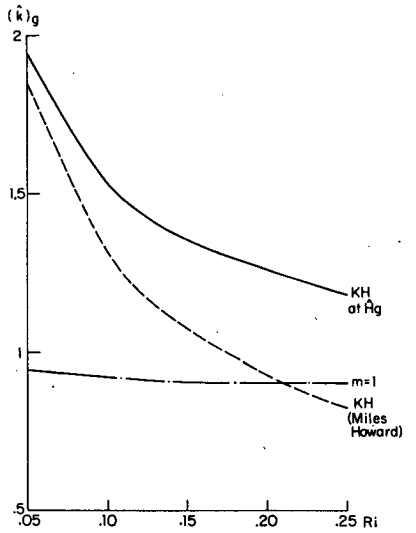

FIG. 15. Wavenumbers of the most unstable (for all $\hat{H}$ and $\hat{k}$) gravity wave mode (i.e., M = 1) as a function of the Richardson number in the shear zone. Also shown are the wavenumbers of the most unstable Kelvin-Helmholtz instability at $\hat{H}_g$ and the wavenumber of the most unstable Kelvin-Helmholtz instability for a slightly different model with no stratification outside the shear zone in an unbounded fluid (Miles and Howard, 1964).

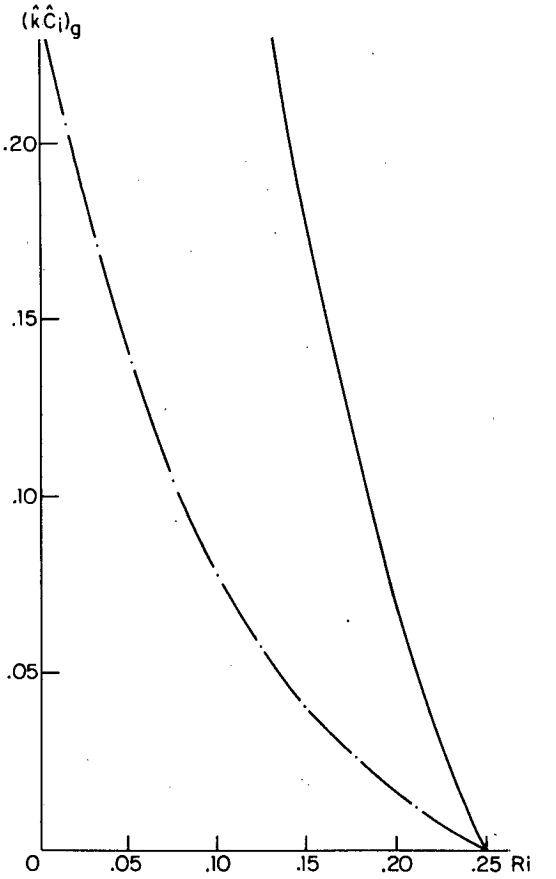

FIG. 16. Maximal growth rates, $(\hat{k}\hat{c}_i)_g$, for all $\hat{H}$ and $\hat{k}$, of gravity wave instabilities as a function of Ri. Also shown are the maximal growth rates of Kelvin-Helmholtz instabilities, for all $\hat{k}$, at $\hat{H}_g$.

stabilities. One such profile consisting of a constant $\bar{u}_z$ and variable N^2 was described by Lindzen *et al.* (1980). The details of this case are presented in a subsequent article (Rosenthal and Lindzen, 1983). Kelvin–Helmholtz instabilities can be suppressed relative to gravity wave instabilities when low Richardson number layers arise from layers of reduced static stability rather than layers of enhanced shear—the latter being essential to the existence of vorticity waves.

5. Concluding remarks

We have shown that gravity wave instabilities associated with concentrated shear zones having Richardson numbers greater than 0 have growth rates that are maximized at particular values of nondimensional ground to shear layer distance $\hat{H}$, to an extent less pronounced than found by Lindzen and Rosenthal (1976) for shear layers having Ri = 0, but still clearly noticeable. In observations made away from the shear layer such as those of Hooke *et al.* (1973) using a ground-based microbarograph array, observed wavelengths are close to those of the most unstable gravity wave. Also, layered structures observed to be associated with shear zones (Ottersten *et al.*, 1973) are more indicative of internal gravity waves than of Kelvin–Helmholtz instabilities, for which exponential decay away from the unstable interface is much greater than for gravity waves. However, after an exhaustive search involving varying the height of the shear zone from the ground and the wavenumber k, we found that, for any Richardson number less than ¼, the growth rates of gravity wave instabilities could be as much as, but not greater than, 26% of the maximal growth rates of Kelvin–Helmholtz instabilities having a critical level with the same Richardson number as the gravity wave instabilities have. Even though the relative importance of gravity wave instabilities is significantly greater than found by other investigators (e.g., Davis and Peltier, 1976), the largest growth rates are still associated with Kelvin–Helmholtz instabilities.

In order to determine if shear profiles in the atmosphere could exist with gravity waves rather than Kelvin–Helmholtz instabilities predominating, it is helpful to consider differences between the models considered by Davis and Peltier (1976) and by us which could account for their not finding as large gravity wave growth rates as a function of Ri as we do. As explained in Section 4, one reason for the relative unimportance of gravity waves in the model considered by Davis and Peltier is that in the tanh-velocity profile they consider, the Richardson number at critical levels for gravity waves is generally greater than the Richardson number at the critical level for Kelvin–Helmholtz instabilities. Another important reason is that the large temperature gradient they assume to exist around the inflection point in the wind

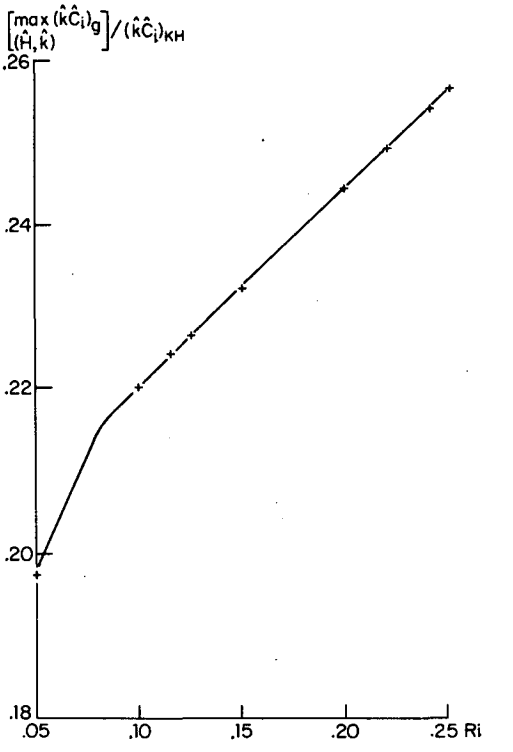

FIG. 17. Ratio of maximal growth rate, for all $\hat{k}$ and $\hat{H}$, of gravity wave instabilities to that of Kelvin–Helmholtz instabilities, for all $\hat{k}$ at $\hat{H}_K$, as a function of Ri.

profile makes the Brunt–Väisälä frequency have a local maximum there, whereas we now consider a profile with constant Brunt–Väisälä frequency. As explained by Rosenthal (1981), gravity wave growth rates can be enhanced relative to Kelvin–Helmholtz growth rates in profiles with a relative minimum of the Brunt–Väisälä frequency near the critical level in the wind profile. A large density stratification around the inflection point, as considered by Davis and Peltier (1976), decreases the relative growth rates of gravity wave instabilities. Observations of Ottersten *et al.* (1973) (in which a wavelength was measured close to that now calculated for the most unstable gravity wave) show a relative minimum in the Brunt–Väisälä frequency in a well-mixed layer resulting around the critical level. Thus, it is more realistic to take the Brunt–Väisälä frequency to be the same near the critical level as elsewhere (as done now) or smaller near the critical level than elsewhere [as done by Rosenthal and Lindzen (1983) for a velocity profile without two regions of large vorticity gradient in which Kelvin–Helmholtz instabilities (vorticity waves) are absent and only gravity-wave instabilities are present] in order for a model to simulate gravity waves being observable in stratified shear flow.

Acknowledgments. The authors wish to acknowledge the support of the National Science Foundation

under Grant ATM-78-23330 at Harvard and Grant ATM-802-3523 at M.I.T., and the National Aeronautics and Space Administration under Grant NGL-22-007-228.

REFERENCES

Atlas, D., J. I. Metcalf, J. H. Richter and E. E. Gossard, 1970: The birth of "CAT" and microscale turbulence. *J. Atmos. Sci.*, **27**, 903–913.

Booker, J. R., and F. P. Bretherton, 1967: The critical layer for internal gravity waves in a shear flow. *J. Fluid Mech.*, **27**, 513–539.

Davis, P. A., and W. R. Peltier, 1976: Resonant parallel shear instability in the stably stratified planetary boundary layer. *J. Atmos. Sci.*, **33**, 1287–1300.

——, and ——, 1977: Effects of dissipation on parallel shear instability near the ground. *J. Atmos. Sci.*, **34**, 1868–1884.

——, and ——, 1979: Some characteristics of the Kelvin–Helmholtz and resonant overreflection modes of shear flow instability and of their interaction through vortex pairing. *J. Atmos. Sci.*, **36**, 2394–2412.

Goldstein, S., 1931: On the stability of superposed streams of fluids of different densities. *Proc. Roy. Soc. London*, **A132**, 524–548.

Hazel, P., 1972: Numerical studies of the stability of inviscid stratified shear flows. *J. Fluid Mech.*, **51**, 39–61.

Hooke, W. H., F. F. Hall and E. E. Gossard, 1973: Observed generation of an atmospheric gravity wave by shear instability in the mean flow of the planetary boundary layer. *Bound.-Layer Meteor.*, **5**, 29–41.

Howard, L. N., 1961: Note on a paper of John W. Miles. *J. Fluid Mech.*, **10**, 509–512.

Jones, W. L., 1968: Reflexion and stability of waves in stably stratified fluids with shear flow: A numerical study. *J. Fluid Mech.*, **34**, 609–624.

Lindzen, R. S., 1974: Stability of a Helmholtz velocity profile in a continuously stratified, infinite Boussinesq fluid—Applications to clear air turbulence. *J. Atmos. Sci.*, **31**, 1507–1514.

——, and A. J. Rosenthal, 1976: On the instability of Helmholtz velocity profiles in stably stratified fluids when a lower boundary is present. *J. Geophys. Res.*, **81**, 1561–1571.

——, B. Farrell and K. K. Tung, 1980: The concept of wave overreflection and its application to baroclinic instability. *J. Atmos. Sci.*, **37**, 44–63.

Miles, J. W., 1961: On the stability of heterogeneous shear flows. *J. Fluid Mech.*, **10**, 496–508.

——, and L. N. Howard, 1964: Note on a heterogeneous shear flow. *J. Fluid Mech.*, **20**, 331–336.

Ottersten, H., K. R. Hardy and C. G. Little, 1973: Radar and sodar probing of waves and turbulence in statically stable clear-air layers. *Bound.-Layer Meteor.*, **4**, 47–89.

Peltier, W. R., J. R. Hallé and T. L. Clark, 1978: The evolution of finite amplitude Kelvin–Helmholtz billows. *Geophys. Astrophys. Fluid Dyn.*, **10**, 53–87.

Rosenthal, A. J., 1981: Gravity-wave and Kelvin–Helmholtz instabilities in stably stratified shear flows. Ph.D. thesis, Harvard University, 331 pp.

——, and R. S. Lindzen, 1983: Instabilities in stratified shear flow in the absence of Kelvin–Helmholtz instabilities. Submitted to *J. Atmos. Sci.*,

Walsh, G. R., 1975: *Methods of Optimization.* Wiley-Interscience, 200 pp.